
Article:
Fatah, J.M., Harrison, P., Stirner, T. et al. (1998) Double crystal x-ray diffraction simulations of diffusion in semiconductor microstructures. Journal of Applied Physics, 83 (8). pp. 4037-4041. ISSN: 1089-7550

https://doi.org/10.1063/1.367159

Double crystal x-ray diffraction simulations of diffusion in semiconductor microstructures

J. M. Fatah, P. Harrison,[a] T. Stirner,[b] J. H. C. Hogg, and W. E. Hagston
Department of Physics, University of Hull, Hull HU6 7RX, United Kingdom

(Received 17 July 1997; accepted for publication 23 December 1997)

Diffusion in group IV, III-V and II-VI semiconductors is an interesting problem not only from a fundamental physics viewpoint but also in practical terms, since it could determine the useful lifetime of a device. Any attempt to control the amount of diffusion in a semiconductor device, whether it be a quantum well structure or not, requires an accurate determination of the diffusion coefficient. The present theoretical study shows that this could be achieved via x-ray diffraction studies in quantum well structures. It is demonstrated that the rocking curves of single quantum wells are not sensitive to diffusion. However the intensity of the first order satellite, which is characteristic of superlattice rocking curves, is strongly dependent upon diffusion and it is proposed that this technique could be used to measure the diffusion coefficient D. © *1998 American Institute of Physics.* [S0021-8979(98)01608-9]

I. INTRODUCTION

Diffusion has been studied in bulk semiconductors for many years[1]. The use of diffusion in the post-growth fine tuning of devices based on semiconductor microstructures has become increasingly important.[2,3] Diffusion could also play an important role in the viability of devices from the viewpoint of their operating properties. In particular diffusion of an alloy component such as Al in GaAs–$Ga_{1-x}Al_xAs$, Mn in CdTe–$Cd_{1-x}Mn_xTe$ or S in ZnSe–ZnS_xSe_{1-x} will affect the optoelectronic properties of the device and could ultimately render the device useless. Hence from the viewpoint of both device fabrication and device stability quantitative knowledge of the amount of diffusion is essential if they are to be optimized and controlled, respectively.

Certain probes of diffusion have already been suggested, such as the excitonic optical properties of quantum well structures[4] and, for the diffusion of a magnetic ion (e.g., Mn^{2+}), the polaronic properties.[5] While the polaronic properties in a magnetic field could offer an accurate measure of the diffusion coefficient of a magnetic ion, they are obviously limited to diluted magnetic semiconductors. Similarly, although the excitonic optical properties of nonmagnetic materials could be employed successfully to investigate diffusion, they would probably need to be used in conjunction with another technique, such as x-ray diffraction, in order to reduce any uncertainties in quantum well widths, etc.

In the present theoretical work it will be demonstrated that semiconductor quantum well structures offer a unique environment for probing diffusion. In particular it is shown that computer simulations of double crystal x-ray diffraction (DCXRD) curves for annealed multiple-quantum well structures, in conjunction with the corresponding experimental data, can provide an accurate measure of the diffusion constant of an alloy constituent in all of the technologically significant group IV, III-V and II-VI semiconductors.

II. COMPUTER SIMULATION

To interpret the rocking curves resulting from x-ray diffraction studies of crystals and to obtain accurate values for various structural parameters (such as the alloy concentration x, the degree of lattice relaxation, etc.) it is important to carry out a profile simulation.[6] This profiling can be done by simulating the diffraction of x rays from crystals using the dynamical x-ray diffraction theory, reviews of which are given in Refs. 7 and 8. The problem is to solve Maxwell's equations in a medium which has a complex, triply periodic electric susceptibility χ. In the x-ray case only two waves with appreciable amplitudes are normally allowed to exist within the crystal. These two, the incident and diffracted waves, are described by the wave vectors $\mathbf{K}_0$ and $\mathbf{K}_h$, and are connected to the reciprocal lattice vector $\mathbf{h}$ by the Laue equation

$$\mathbf{K}_0+\mathbf{K}_h=\mathbf{h}. \tag{1}$$

The solution, Equation (2), defines the dispersion surface, which is the locus of the end points of the allowable wave vectors inside the crystal.

$$\alpha_0\alpha_h=\tfrac{1}{4}C^2k^2\chi_h\chi_{\bar{h}}. \tag{2}$$

Here C is the polarization factor, $k=|\mathbf{K}_0|=|\mathbf{K}_h|=1/\lambda$ (at the wavelength λ) and α_0 and α_h are given by

$$\alpha_0=\frac{1}{2k}[\mathbf{K}_0.\mathbf{K}_0-k^2(1+\chi_0)]$$

$$\alpha_h=\frac{1}{2k}[\mathbf{K}_h.\mathbf{K}_h-k^2(1+\chi_0)].$$

The total wavefield D_{tot} is related to the amplitudes of the direct and diffracted waves, D_0 and D_h, by

[a]Present address: Dept. of Electron. and Electron. Eng., University of Leeds, Leeds LS2 9JT, U.K.
[b]Electronic mail: t.stirner@physics.hull.ac.uk

$$D_{tot}=\sum_{j=1}^{2}\left[D_{0j}\exp(-2\pi i\mathbf{K}_{0j}.\mathbf{r})+D_{hj}\exp(-2\pi i\mathbf{K}_{hj}.\mathbf{r})\right].$$

The amplitude ratio $X'(=D_h/D_0(z))$ is given by the relation

$$X'=\frac{2\alpha_0}{kC\chi_{\bar{h}}}=\frac{kC\chi_h}{2\alpha_h}.$$

The relative strengths of the direct and diffracted beams emerging from the perfect crystal thus depend on α_0 and α_h, which in turn depend on the deviation $\Delta\Theta$ of the incident beam from the exact Bragg angle. Thus as the crystal is rotated, the diffracted intensity changes, giving the rocking curve its finite width.

The generalized diffraction theory, developed by Takagi[9] and Taupin,[10] can be used to describe the passage of x-rays through a crystal with any type of lattice distortion. In the two-beam approximation the wavefield inside the crystal can be described by two coupled first order partial differential equations expressed along the depth z into the crystal

$$\frac{i\lambda}{\pi}\gamma_0\frac{\partial D_0}{\partial z}=\chi_0 D_0+C\chi_{\bar{h}}D_h, \tag{3}$$

$$\frac{i\lambda}{\pi}\gamma_h\frac{\partial D_h}{\partial z}=(\chi_0-\alpha_h)D_h+C\chi_h D_0, \tag{4}$$

where χ_h is related to the structure factor F_h, the electron radius r_e and the unit cell volume V by

$$\chi_h=\frac{\lambda^2 r_e}{\pi V}F_h.$$

γ_0 and γ_h are the direction cosines of the incident and reflected beams relative to the inward surface normal. The parameter α_h, which represents the deviation of the incident wave from the exact Bragg condition, is given by

$$\alpha_h(\omega)=-2\frac{\lambda}{d}\Delta\Theta_h\cos(\Theta_B),$$

where $\Delta\Theta_h$ is the local deviation from the exact Bragg angle, taking lattice strains into account, Θ_B is the local exact Bragg angle and d is the interplane spacing.

Equations (3) and (4) can now be combined, by defining an amplitude ratio $X'=D_h/D_0(z)$, and integrated.[11] We thus obtain the amplitude ratio $X(Z)$

$$X(Z,\omega)=\frac{X'(z,\omega)S+i(BX'(z,\omega)+E)\tan(DS[z-Z])}{S-i(AX'(z,\omega)+B)\tan(DS[z-Z])}, \tag{5}$$

where the variable z is the depth above the depth Z at which the amplitude ratio is the known value X'. In Equation (5) we use the parameters[11]

$$A=\frac{|\gamma_h|}{\gamma_0}\chi_{\bar{h}}$$

$$B=\frac{1}{2}\left[\left(1-\frac{|\gamma_h|}{\gamma_0}\right)\chi_0-\alpha_h(\omega)\right]$$

$$D=-\frac{\pi}{\lambda|\gamma_h|}$$

$$E=\chi_h$$

and

$$S=\sqrt{B^2-AE}.$$

To calculate the diffraction profile we need to establish a starting amplitude ratio (chosen as zero deep inside the crystal) and progress up through the crystal layers, and use the amplitude ratio at the top of one layer as the start value for the bottom of the next. This procedure is then repeated for each step in the crystal rotation angle ω.

In the present work interest is focused upon the Cu K_{α_1} 004 rocking curve. To be definite, a quantum well stack which was commensurate with, and grown upon, a 001 InSb substrate with a 1000 Å CdTe buffer layer was employed in the model calculations.

For the purposes of the simulation of rocking curves, quantum well structures can be described completely in terms of alternating layers of material. In the present case $Cd_{1-x}Mn_xTe$ layers were assumed, with differing alloy concentrations x. When one of the alloy constituents has diffused (i.e., Mn), a more complex variation of x along the growth (z) axis occurs. In order to model the latter it is assumed, for the purpose of illustration, that the diffusion coefficient D does not vary with the alloy concentration x. This leads to Fick's second law in one dimension,

$$\frac{\partial x}{\partial t}=\frac{\partial}{\partial z}D\left(\frac{\partial x}{\partial z}\right), \tag{6}$$

which has been described in detail in an earlier publication.[4]

Various standard solutions to the linear case of Fick's second law do exist,[12,13] depending on the initial distribution of the diffusing substance. For the following calculations, Crank's[12] solution to the diffusion equation for a source with an extended initial distribution has been employed. Using x_o for the initial concentration of the diffusing substance, Crank's equation reads

$$x=\frac{x_o}{2}\operatorname{erfc}\left(\frac{z}{2\sqrt{Dt}}\right), \tag{7}$$

where erfc denotes the complementary error function. The supposed linearity of Fick's second law, i.e., the constancy of the diffusion coefficient D, now allows a linear superposition of the separate solutions to the diffusion equations at any given time t.

It should also be pointed out that the following calculations are not microscopic in the sense that there is no reference to impurity atoms or lattice defects, such as interstitials or vacancies (which can enhance diffusion processes dramatically). For such a calculation, which takes impurities and lattice defects into account, a diffusion Monte Carlo

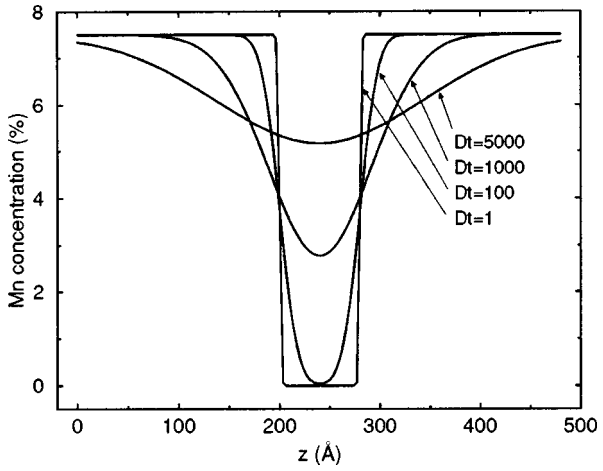

FIG. 1. Diffusion profiles for a single CdTe well of width 80 Å, surrounded by $Cd_{0.925}Mn_{0.075}Te$ barriers, for various values of Dt (in $Å^2$).

analysis would be necessary. However, the macroscopic model employed is of proven utility for abstracting information from experimental data.[14]

Figure 1 shows diffusion profiles for a single CdTe well of width 80 Å, surrounded by 200 Å $Cd_{0.925}Mn_{0.075}Te$ barriers, in which the diffusion is due entirely to a post-growth anneal. As a linear diffusion process has been assumed the curves are universal, i.e., the diffusion coefficient and the time are interchangeable. Hence the separate graphs are labelled with the corresponding product of diffusion coefficient D and time t (in units of $Å^2$). For example, if we assume for the graph with the largest amount of diffusion a diffusion coefficient of $D=0.1$ $Å^2/s$ we obtain, by using the Dt value of 5000 $Å^2$, a corresponding annealling time of $t=50\,000$ $s \approx 14$ h.

III. RESULTS AND DISCUSSION

A. Diffusion of single quantum wells

Figure 2 shows the simulated rocking curves for the single quantum well structures of Fig. 1. Note that for the purpose of clarification the curves have been scaled. It is clear that the central (substrate) peak dominates and, at first

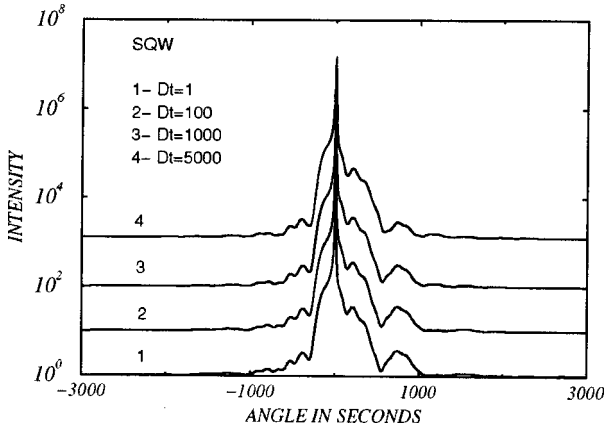

FIG. 2. Simulated Cu K_{α_1} 004 DCXRD rocking curves for the single quantum wells of Fig. 1.

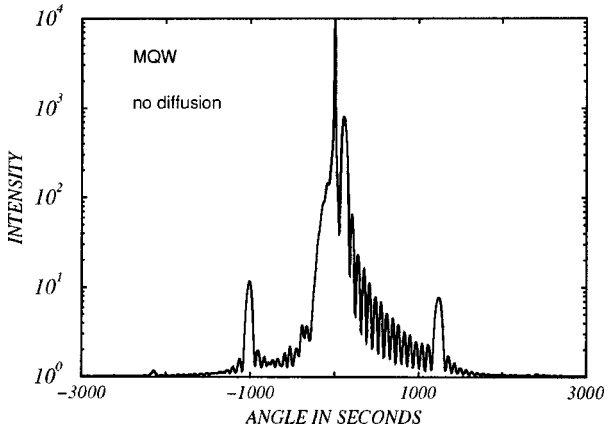

FIG. 3. Simulated Cu K_{α_1} 004 DCXRD rocking curve for 15×80 Å CdTe wells separated by 80 Å $Cd_{0.925}Mn_{0.075}Te$ barriers with no diffusion.

sight, the curves are virtually identical, even though the quantum wells themselves are significantly different. Subtle differences between the curves do exist in the peak centred around 700–800 arcsec, but they are far too small to be detectable with any reliability by experiment. In summary, single quantum wells are of limited utility from the viewpoint of DCXRD studies for the investigation of diffusion.

B. Diffusion of superlattices

It is envisaged that superlattices could be a more sensitive measure of diffusion, since the additional periodicity of the superlattice unit cell leads to a strong feature (i.e., the superlattice satellites) on the rocking curve, which is characteristic of the exact form of the structure. In particular the angular separation of the first order satellite from the substrate peak is a measure of the superlattice period. Furthermore, the height and width of the peak give an indication of the number of repeats and uniformity of the periodicity.

Figure 3 displays the simulated rocking curve (of the sample described in Fig. 4 below) with no diffusion. It is clear from this figure that the first order satellite peaks are an order of magnitude larger than the second order ones. From an experimental viewpoint, this means that it is much more

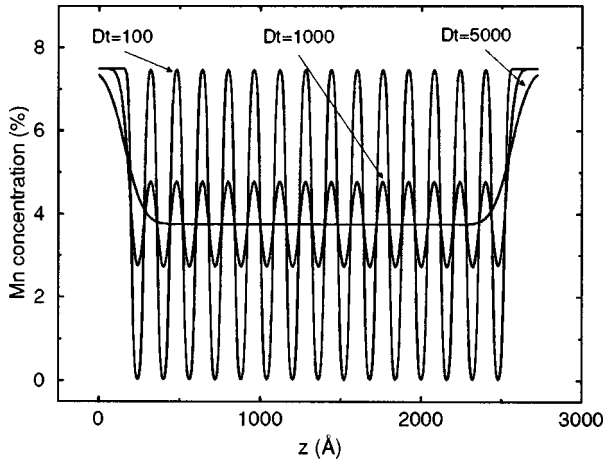

FIG. 4. Diffusion profiles for the sample of Fig. 3 with varying values of Dt (in $Å^2$).

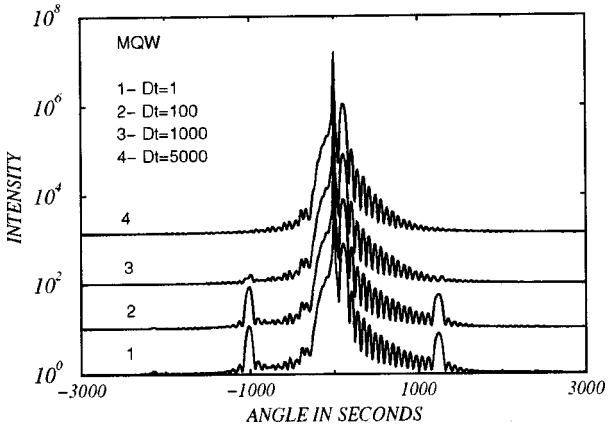

FIG. 5. Simulated rocking curves for the superlattices of Fig. 4 with differing amounts of diffusion (Dt in units of Å^2).

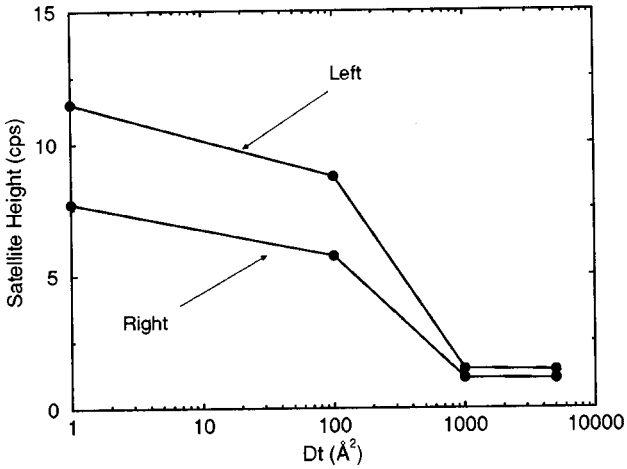

FIG. 6. Peak intensity of the first order superlattice satellites of Fig. 5 as a function of the amount of diffusion Dt.

difficult to monitor accurately the changes in the second order satellites. Hence although the latter are sensitive to the well shape[15] we will focus our attention in the present paper on the first order satellites which can be more accurately monitored experimentally.

For comparison with the previous section, the superlattice was chosen to have 15 80 Å CdTe wells, separated by 80 Å $Cd_{0.925}Mn_{0.075}Te$ barriers, with 200 Å outer barriers. Employing the same Dt values as in Section III A, the manganese concentration x as a function of distance z along the growth direction is displayed in Fig. 4.

The simulated rocking curves for the superlattices of Fig. 4 are shown in Fig. 5. Although the first order superlattice satellites are clearly visible in the bottom curve of Fig. 5 at angles of $\approx -1000''$ and $+1200''$, for increasing amounts of diffusion these satellite peaks are eroded away, while the rest of the curves remain virtually unaltered. This could have been anticipated *a priori* since increasing amounts of diffusion in a superlattice would lead eventually to a uniform alloy (as shown in the $Dt = 5000$ Å^2 curve of Fig. 4), which would contain no superlattice periodicity and hence no superlattice satellites would be observed. The diffusion profiles displayed in Fig. 4 clearly represent intermediaries between the two extremes of a square well superlattice and an alloy.

The intensity of both first order superlattice satellites are plotted as a function of Dt in Fig. 6. It can be seen that the intensities are a sensitive function of the amount of diffusion; in this case the peaks decrease by about a factor of 10 from the superlattice with effectively no diffusion (i.e., $Dt = 1$ Å^2) to that with considerable diffusion (i.e., $Dt = 5000$ Å^2). As the annealling time in any post-growth process is easily measured, then Fig. 6 demonstrates that DCXRD could be used to measure the diffusion coefficient D for any particular annealing temperature by repetitive measurements on the same sample at successively longer time intervals.

Note that although attention has been focused upon the CdTe–$Cd_{1-x}Mn_xTe$ system, the results are completely general. The technique could be equally applied to Al diffusion in GaAs–$Ga_{1-x}Al_xAs$ or Ge in Si–$Si_{1-x}Ge_x$ strained layer superlattices, by simply growing the appropriate multiple-quantum well structure and performing annealing and x-ray diffraction measurements. In fact, the effects desribed in this section have recently been observed in an experimental x-ray diffraction study of thermally induced disordering in a ZnSSe–ZnSe superlattice system.[16]

C. Diffusion during growth

The conclusions of the previous section are based on the assumption that no diffusion occurs during growth of the superlattice. Depending on the diffusion coefficient (which could be a strongly varying function of the growth temperature) and the total growth time (which itself depends on the growth rate and the overall thickness of the superlattice stack) the amount of diffusion during growth could be significant.

Figure 7 shows the effect of such diffusion during the growth of the superlattice of Section III B, for various values of D (in units of Å^2/s). There is no post-growth annealing, hence the last well to be grown exhibits virtually no diffusion, while the first well can exhibit significant diffusion. In these calculations the growth rate was chosen to have the typical value of 1.83 Å/s. The curves are no longer universal, hence the diffusion coefficient D has been chosen to repre-

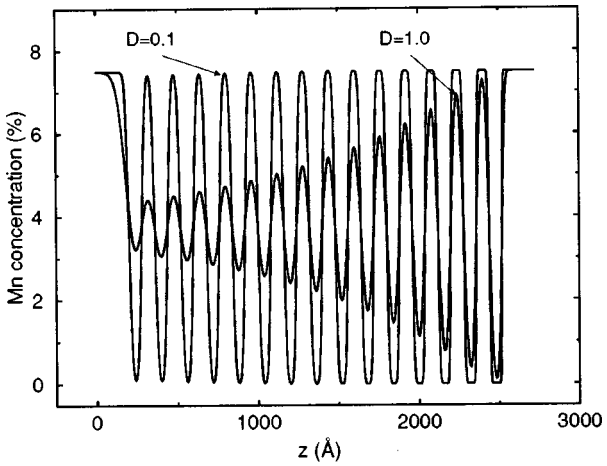

FIG. 7. Superlattice of Fig. 3 with diffusion during growth only (D in units of Å^2/s).

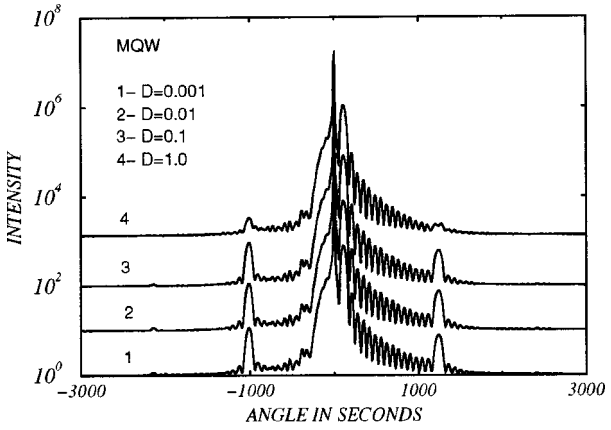

FIG. 8. Simulated rocking curves for the superlattices of Fig. 7 (D in units of Å^2/s).

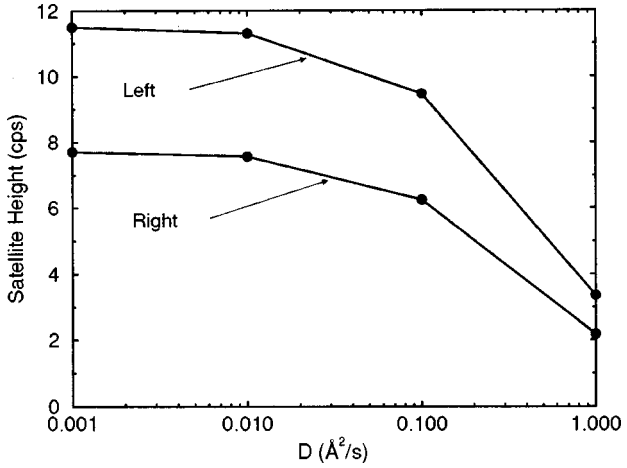

FIG. 9. Peak intensity of the first order superlattice satellites of Fig. 8 as a function of the diffusion coefficient D.

sent the extremes of hardly any diffusion ($D=0.001$ Å^2/s) to almost total destruction of the first well grown ($D=1$ Å^2/s). Note that only curves for $D=0.1$ and 1 Å^2/s are shown for clarity. The diffusion time t for the first layer is now set as the growth time, i.e.,

$$t=\frac{\text{total thickness of superlattice stack}}{\text{growth rate}}=\frac{2720\ \text{Å}}{1.83\ \text{Å/s}}\approx 25\ \text{min}.$$

Clearly the diffusion time decreases to zero for the last layer in the stack and takes on intermediate values between these two limits for different layers. Figure 8 illustrates the dynamical simulation of the x-ray rocking curves of the superlattices of Fig. 7, together with those appropriate to $D=0.01$ and 0.001 Å^2/s. As in Section III B, the rocking curves remain virtually unaltered except for the first order superlattice satellites at $\approx -1000''$ and $+1200''$, which are dramatically reduced. This is not due specifically to a loss of superlattice periodicity, but to a reduction in the difference between well and barrier material, as the earliest grown wells tend towards alloys, as shown in Fig. 7.

Figure 9 summarizes the changes in the satellite peak intensities for both left ($\approx -1000''$) and right ($\approx +1200''$) first order peak. Hence, the amount of diffusion occurring during growth can be deduced by comparison of the simulation of the experimentally measured rocking curve, with the simulation of the ideal (i.e., undiffused) rocking curve. The growth conditions can then be adjusted accordingly to control such processes.

IV. CONCLUSION

It has been demonstrated that multiquantum well structures offer an invaluable means of measuring the diffusion coefficient of any semiconductor. Simulations of DCXRD rocking curves cannot only be utilized to quantify the diffusion occurring in post-growth annealling, but can also be used to determine the amount of diffusion occurring *during* growth of semiconductor heterostructures.

ACKNOWLEDGMENT

The authors would like to thank EPSRC (U.K.) for financial support.

[1] D. Shaw, J. Cryst. Growth **86**, 778 (1988).
[2] K. Meehan, P. Gavrilok, N. Holonyak, R. D. Burnham, and R. L. Thornton, Appl. Phys. Lett. **46**, 75 (1985).
[3] K. P. Homewood, B. L. Weiss, and A. C. Wismayer, Semicond. Sci. Technol. **4**, 472 (1989).
[4] P. Harrison, W. E. Hagston, and T. Stirner, Phys. Rev. B **47**, 16 404 (1993).
[5] T. Stirner, W. E. Hagston, P. Harrison, and J. P. Goodwin, J. Appl. Phys. **75**, 3466 (1994); T. Stirner, P. Harrison, and W. E. Hagston, *ibid.* **77**, 1314 (1995).
[6] J. H. C. Hogg, J. E. Nicholls, S. R. Jackson, W. E. Hagston, D. E. Ashenford, B. Lunn, and S. Ali, Mater. Sci. Eng. B **16**, 60 (1993).
[7] B. W. Batterman and H. Cole, Rev. Mod. Phys. **36**, 681 (1964).
[8] Z. G. Pinsker, *Dynamical Scattering of X-rays in Crystals* (Springer, New York, 1978).
[9] S. Takagi, Acta Crystallogr. **15**, 1311 (1962); J. Phys. Soc. Jpn. **26**, 1239 (1969).
[10] D. Taupin, Bull. Soc. Fr. Mineral. Cristallogr. **87**, 469 (1964).
[11] P. F. Fewster, J. Appl. Crystallogr. **25**, 714 (1992); P. F. Fewster and C. J. Curling, J. Appl. Phys. **62**, 4154 (1987).
[12] J. Crank, *Mathematics of Diffusion* (Oxford University Press, Oxford, 1957).
[13] P. Shewmon, *Diffusion in Solids* (McGraw-Hill, New York, 1963).
[14] W. P. Gillin, K. P. Homewood, L. K. Howard, and M. T. Emeny, Superlattices Microstruct. **9**, 39 (1991).
[15] J. H. C. Hogg, A. Bairstow, G. W. Mathews, D. Shaw, and J. D. Stedman, Mater. Sci. Eng. B **16**, 195 (1993); J. H. C. Hogg, D. Shaw, and D. M. Staudte, Appl. Surf. Sci. **50**, 87 (1991); R. N. Fleming, D. B. McWhan, A. C. Gossard, W. Wiegmann, and R. A. Logan, J. Appl. Phys. **51**, 337 (1980).
[16] M. Kuttler, M. Grundmann, R. Heitz, U. W. Pohl, D. Bimberg, H. Stanzel, B. Hahn, and W. Gebhardt, J. Cryst. Growth **159**, 514 (1996).